ACS OMEGA

http://pubs.acs.org/journal/acsodf

Article

Poly(3,4-ethylenedioxythiophene):Polystyrene Sulfonate-Modified Electrode for the Detection of Furosemide in Pharmaceutical Products

Md. Shamim Hossain, Md. Abdul Khaleque, Md. Romzan Ali, Md. Sadek Bacchu, Md. Ikram Hossain, Mohamed Aly Saad Aly, and Md. Zaved Hossain Khan*

Cite This: *ACS Omega* 2023, 8, 16851−16858

Read Online

ACCESS | Metrics & More | Article Recommendations

ABSTRACT: Furosemide (4-chloro-2-(furan-2-ylmethylamino)-5-sulfamoyl benzoic acid) is a widely used, FDA-approved drug prescribed for several symptoms associated with heart, kidney, liver failure, or chronic high blood pressure. In this work, a glassy carbon working electrode modified with poly(3,4-ethylenedioxythiophene):polystyrene sulfonate is developed to detect furosemide (FURO) with high sensitivity and precise selectivity. The modified electrode was also characterized using field emission scanning electron microscopy, attenuated total reflectance−Fourier transform infrared, and cyclic voltammetry. Here, an efficient and cost- and time-efficient technique to study the furosemide mechanism of reaction in an acidic liquid medium is presented. An electrochemical oxidation of loop diuretic furosemide was investigated in a supporting electrolyte, 0.01 M of phosphate buffer (at a pH level of 4.0) at 25 ± 0.1 °C using a differential pulse voltammetric (DPV) technique. Under optimized parameters, the developed sensor displays a wide detection range of furosemide concentrations of 6.0×10^{-6} to 1.0×10^{-4} M with a detection limit of 2.0×10^{-6} M using DPV. The presented sensor offers a robust and high-precision technique with an excellent reproducibility to detect furosemide in as a real sample such as urine and pharmaceutical products.

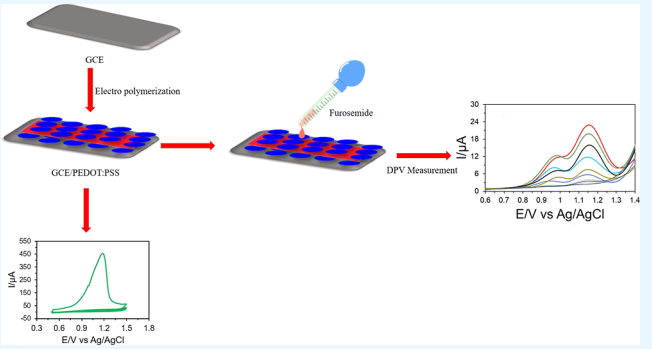

1. INTRODUCTION

Furosemide is a sulfonamide chemically known as 4-chloro-2-(furan-2-ylmethylamino)-5-sulfamoylbenzoic acid.[1] Furosemide is a widely used, FDA-approved drug with diuretic properties, allowing it to become a useful medicine for treating dropsical condition related to cardiac arrest, chronic renal failure,[2,3] congestive heart failure, hypertension,[4] and liver related diseases.[5] Furthermore, furosemide is commonly used as a doping agent in sport-related applications.[1] Furosemide can be rapidly absorbed with oral intake, showing a great diuretic effect in a short time.[6] Literature revealed that the bioavailability of furosemide ranges from 60 to 70% with a plasma half-life of about 1−2 h.[7] Furthermore, the aqueous solubility of furosemide is fairly poor; however, it has high efficacy due to its inhibitory effect on sodium chloride (NaCl)/potassium chloride (KCl)/chloride (2Cl) cotransporter in the ascending limb of the loop of Henle.[8] Several methods were reported for the specific discovery of these diuretics in both biological fluids and pharmaceutical preparations. Furosemide is always accompanied with various side effects such as diarrhea, muscle cramps, urination, constipation, and thirst.[9] Moreover, there are severe aftereffects associated with furosemide, including rapid weight loss, fever, dark urine, electrolyte abnormalities, dehydration, nausea, clay-colored stools, jaundices, and vomiting.[9] Recently, furosemide is widely and frequently used in neonatal clinics, and knowing the harmful effects accompanied with the use of furosemide, studying furosemide and investigating its reaction mechanism are urgently required. Furthermore, FURO drug in blood and urine concentrations has an effect on their activity for changing the physiological condition. This study will be helpful for drug dosage formation by the physician.

Furosemide is usually prepared and characterized by liquid chromatography with spectrophotometric,[5,10,11] spectrofluorimetric detection,[12−14] chemiluminescent,[15] and micellar electrokinetic chromatographic methods.[12] These techniques

Received: January 24, 2023
Accepted: April 19, 2023
Published: May 4, 2023

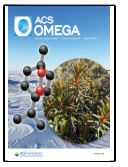

Scheme 1. Schematic Procedure of Formulating GCE/PEDOT:PSS and the Recognition of Furosemide

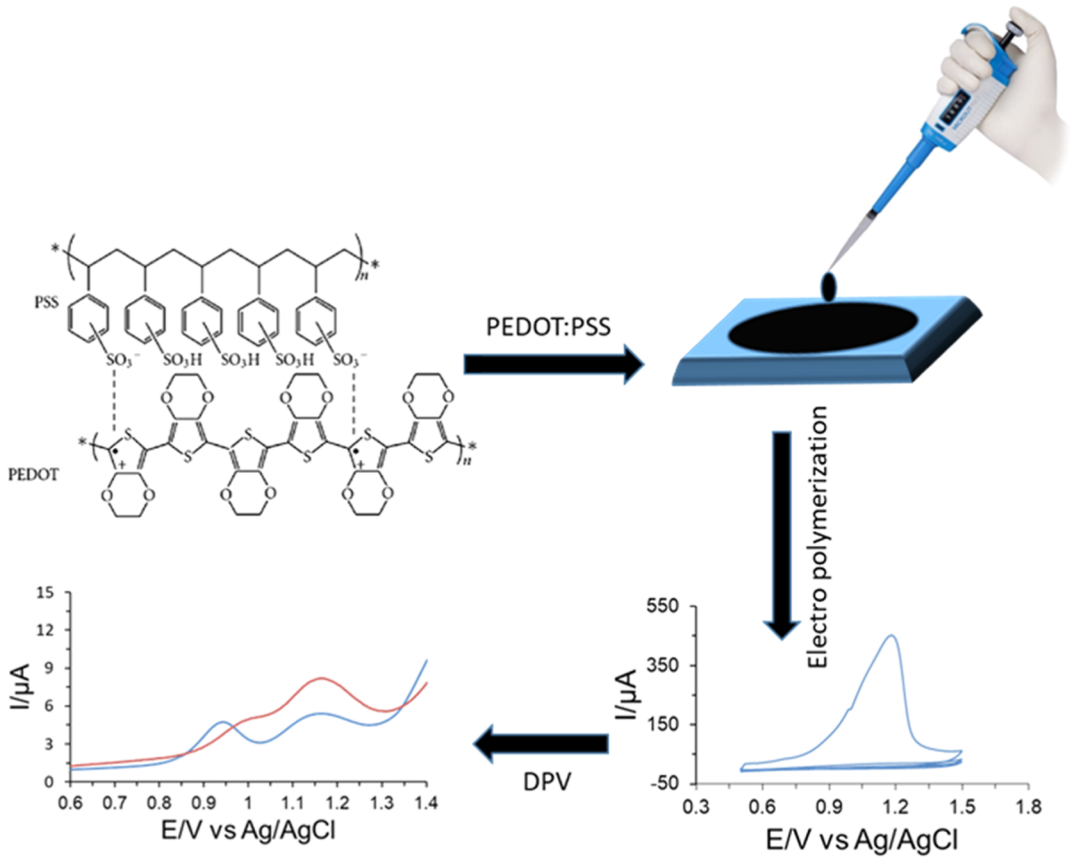

include some extraction steps, and thus, they are time-consuming. It was reported that furosemide was quantified using electrochemical methods by a glassy carbon electrode (GCE),[13] a hanging mercury drop electrode, and a graphite electrode.[16] In this study, GCE is chosen for the outstanding chemical stability and hard and dense behavior. Additionally, the oxidation rate in oxygen, water, and carbon dioxide is lower than in graphite and metal-based electrodes.[17]

Poly(3,4-ethylenedioxythiophene):polystyrene sulfonate (PEDOT:PSS) is a an electrically conductive polymer composed of a mixture of two ionomers. Due to the unique properties of PEDOT:PSS such as ease of processing conductivity, ductility, and transparency, it becomes a benchmark material in various applications within different fields, including field effect transistors, active materials for electrochromic devices (due to the high electrical conductivity, mechanical flexibility, low surface roughness, and low price), thermoelectric materials, antistatic coatings, and electrically conducting coatings.[18−22] Moreover, the PEDOT:PSS film was utilized as an efficient electrode-modifying material for applications in sensors,[23−26] supercapacitors,[27−30] and fuel cells.[31,32]

In the present work, an efficient and reliable electrochemical sensor for the selective and sensitive detection of FURO by modified GCE with PEDOT:PSS polymer was developed. PEDOT:PSS was drop-cast on a GC working electrode to efficiently improve the electrochemical activity of the working electrode. Furthermore, the modified electrode was used to analyze FURO in urine and pharmaceutical samples. The developed biosensor exhibits excellent reproducibility, fast response, high sensitivity, and the capability of detecting other potentially interfering species.

2. MATERIALS AND METHODS

2.1. Chemicals and Materials. Furosemide, PEDOT:PSS solution (1.3 wt % dispersed in water), was purchased from Sigma-Aldrich, China. Ultrapure water (<18.2 U resistivity) was used during the course of the experimental work. 1 mM phosphate-buffered saline (PBS, pH level of 4.0) electrolyte was utilized for all electrochemical measurements. 5 mM $Fe(CN)_6^{3-/4-}$ as a redox probe solution was prepared in 0.1 M KCl for electrode test.

2.2. Fabrication of GCE/PEDOT:PSS. The bare GC working electrode was first mirror-polished with 1, 0.3, and 0.05 μm of alumina slurry on a polishing pad. Next, the cleaned GC working electrode was sonicated in ethanol and deionized water for 5 min each. Then, the surface of the GC working electrode was pretreated with 1 M of sulfuric acid (H_2SO_4) by cyclic voltammetry (CV) using a voltage range of 1.0 to −1.0 V for 23 cycles with an optimum scan rate of 0.1 V s^{-1}. Then, the GCE electrode was washed with ultrapure water and dried under ambient nitrogen. Next, 4 mL of the prepared PEDOT:PSS solution was applied on the precleaned GCE and left to dry in a desiccator at room temperature overnight. The PEDOT:PSS-modified GCE was stored at 4 °C for further use (Scheme 1).

2.3. Apparatus and Instruments. Electrochemical-based experiments were conducted on a CS300 electrochemical workstation (CORRTEST, CS300; Wuhan, China), performing a three-electrode system for voltammetric measurements. The used three-electrode system contained a working

https://doi.org/10.1021/acsomega.3c00463
ACS Omega 2023, 8, 16851−16858

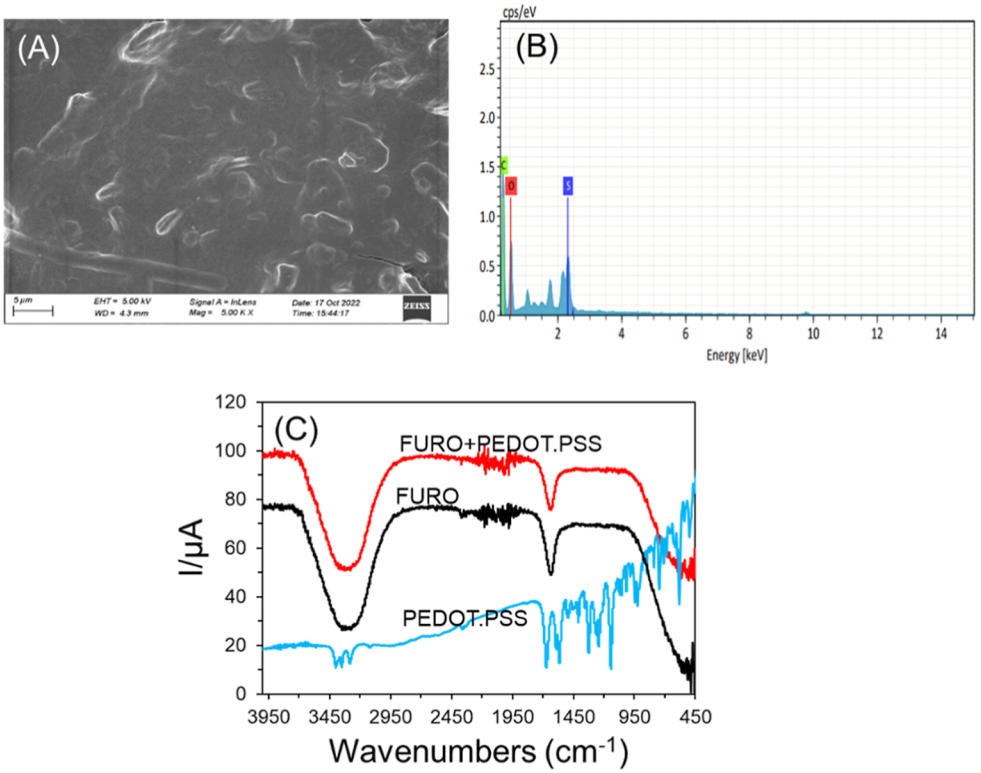

Figure 1. SEM images of (A) bare GCE/PEDOT:PSS; (B) EDX spectra of the PEDOT:PSS modified surfaces, showing the distribution of C, O, and S elements on the PEDOT:PSS-coated surface; and (C) ATR−FTIR spectrum of PEDOT:PSS, FURO, and PEDOT:PSS + FURO.

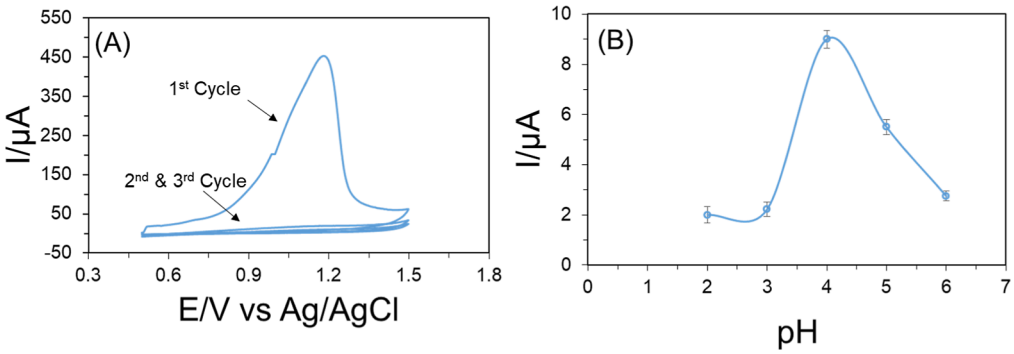

Figure 2. CV experimental results of (A) electropolymerization process in 0.01 M of PBS (at a pH level of 4.0) solution containing 100 μM furosemide and (B) effect of pH level of PBS on the electrochemical signal of the GCE/PEDOT:PSS sensor to detect a 0.1 × 10^{-4} M furosemide.

electrode that is made of coated GCE, reference electrode that is made of silver/silver chloride (Ag/AgCl), and a counter electrode that is made of a platinum wire. The surface morphology of the PEDOT:PSS surface coat was characterized by scanning electron microscopy (SEM) using a ZEISS Gemini SEM 500 model, and transmission electron microscopy was performed with the JEOL 2100 model.

3. RESULTS AND DISCUSSION

3.1. Surface Morphology and Functional Group Study of PEDOT:PSS. The field emission scanning electron microscope was used to characterize the morphology of the prepared electrode surface, and the results are shown in Figure 1. Figure 1A clearly shows the magnified view of the electrode surface composition of PEDOT:PSS. From Figure 2A, it is confirmed that the covalent bond was formed between PEDOT and PSS after electropolymerization. The energy-dispersive X-ray (EDX) surface distributions confirmed the presence of 59.81% C, 33.87% O, and 6.32% S, indicating the surface modification with PEDOT:PSS as shown in Figure 1B.

The attenuated total reflectance−Fourier transform infrared (ATR−FTIR) spectroscopy spectra for PEDOT:PSS, FURO, and a nanocomposite mixture of PEDOT:PSS and FURO are represented in Figure 1C. For the PEDOT:PSS spectrum, the peak was observed at a range of 408.49−1643.35 cm^{-1}. The IR bands in the range of 632.89−1643.35 cm^{-1} are mainly due to C═C, C−C, C−O−C, and C−S stretching of the quinoid structure of the thiophene rings and the sulfonic acid group of PSS. In the composite mixture (PEDOT:PSS + FURO), the peaks representing C═O and −OH (in FURO spectrum) at wavelengths 1673.78 and 1565.01 cm^{-1}, respectively, were diminished by a broad alkaline peak at 1636.90 cm^{-1} of PEDOT:PSS spectrum.[33] Additionally, the remaining wide range of FURO spectra shifted to the vibration modes of

https://doi.org/10.1021/acsomega.3c00463
ACS Omega 2023, 8, 16851−16858

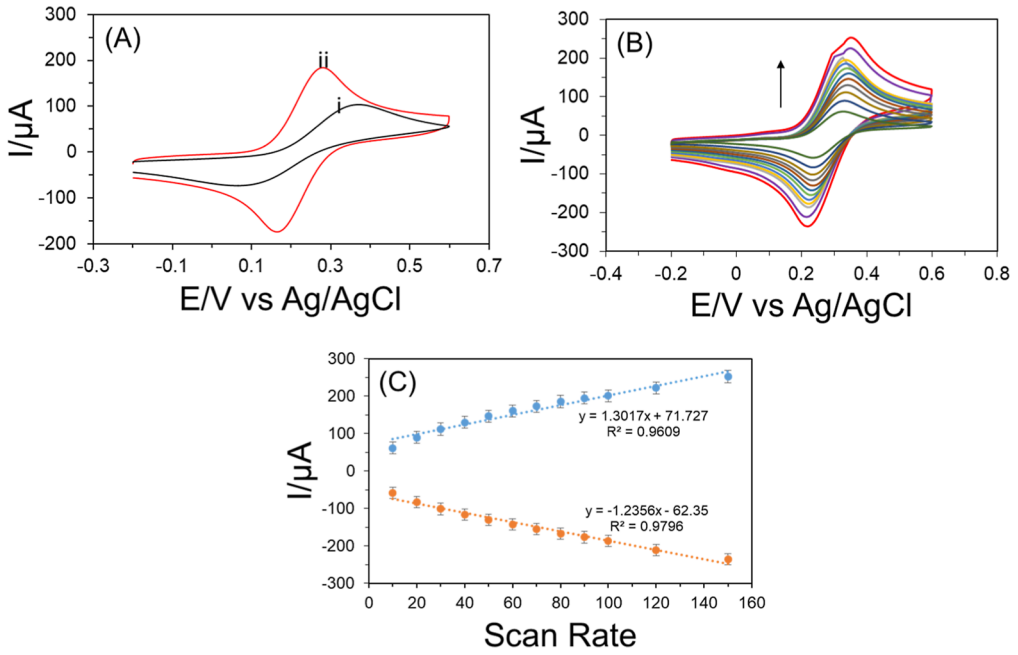

Figure 3. Cyclic voltammograms (A) of the bare GCE (i) and modified GCE/PEDOT:PSS electrodes (ii) measured in 1.0×10^{-4} M of KCl including 5.0×10^{-3} M of $Fe(CN)_6^{3-/4-}$ solution and (B) behavior of the same modified electrode at different scan rates of 10, 20, 30, 40, 50, 60, 70, 80, 90, 100, 120, and 150 mV s^{-1} in the same electrolyte.

Scheme 2. Schematic Procedure of Electrochemical Detection Mechanism of FURO[40]

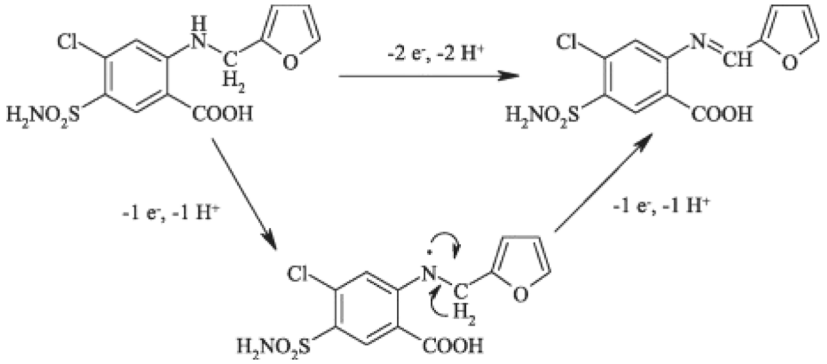

PEDOT:PSS. These bands indicate the pure (without any contamination) nature of PEDOT:PSS even after deposition. FTIR was performed on FURO to detect any sign of interaction, which would be reflected by a change in the position or disappearance of any characteristic stretching vibration of furosemide. The characteristic peaks of furosemide showed N−H stretching at 3400 cm^{-1}, N−H stretching in sulfonamide at 3350 and 3283 cm^{-1}, the C═O stretching and vibration at 1673.78 cm^{-1}, and S═O stretching and vibration at 1142.69 and 1323.70 cm^{-1}, and the most important stretching vibration was OH stretching at 3122 cm^{-1} and NH bending at 1565−1592 cm^{-1}.[34]

GCE/PEDOT:PSS was dipped into 0.01 mol/L PBS (at a pH level of 4.0) solution containing 100 μM FURO, and electropolymerization was performed by CV with a potential range of −0.2 to 0.8 V for three cycles with a scan rate of 100 mV s^{-1} as shown in Figure 2A. Here, the thiophene groups of PEDOT are electropolymerized with sulfonic acid groups of PSS.[35−37] We found that the polymerization process took few cycles to reach the oxidation less state.

The effect of pH level of 0.01 M PBS on the electrochemical signal of the GCE/PEDOT:PSS sensor to detect a 0.1×10^{-4} M FURO was investigated at a pH level range of 2.0−7.4 as can be seen in Figure 2B. It was found that the peak current of the FURO increased with the increase of the pH levels from 2.0 to 4.0, and it decreased for pH levels from 4.2 to 7.4. This indicates that the acidic electrolyte solution is more suitable for FURO oxidation than the alkaline electrolyte solution. It is worth mentioning that the maximum current signal of FURO was achieved at an optimal pH level of 4.0.

3.2. Electrochemical Behavior of GCE/PEDOT:PSS.

Figure 3A shows the electrochemical characterization of the bare GCE and the PEDOT:PSS-modified GCE by CV in 0.1 M KCl including 0.005 M $Fe(CN)_6^{3-/4-}$. From Figure 3A, it can be noted that the lowest peak current with a pair of well-defined redox peaks was obtained for bare GCE with a peak-to-peak separation (ΔE_p) value of 123 mV. Similarly, ΔE_p had a value of 98 mV for GCE/PEDOT:PSS, increasing the diffusion redox rate of $Fe(CN)_6^{3-/4-}$. The electroactive area of GCE/PEDOT:PSS and bare GCE was calculated through using the Randles−Sevcik equation as reported previously.[38,39] The

https://doi.org/10.1021/acsomega.3c00463
ACS Omega 2023, 8, 16851−16858

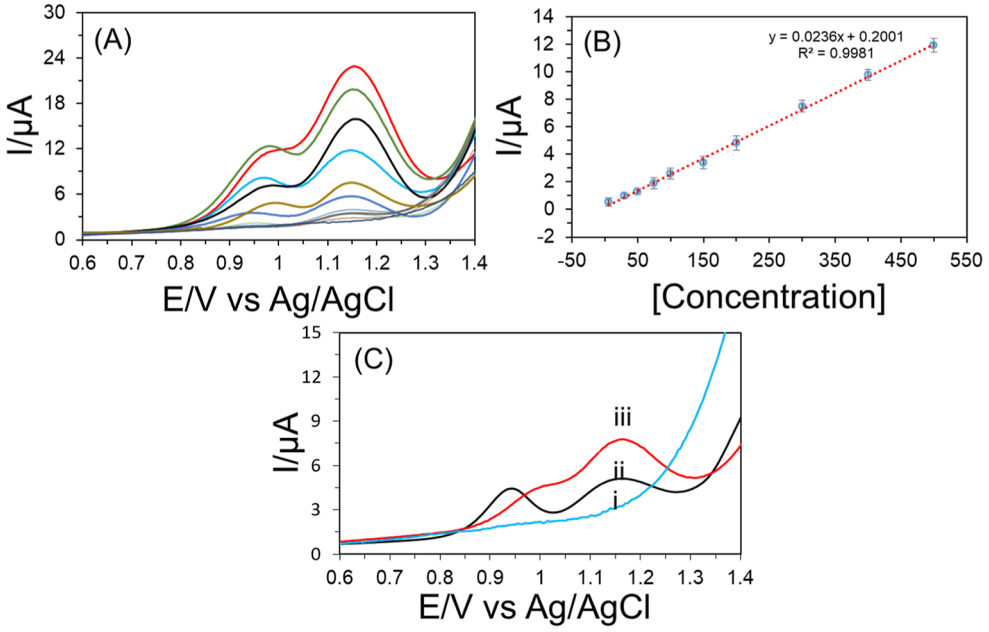

Figure 4. (A) DPV analysis obtained for the determination of FURO using GCE/PEDOT:PSS in a phosphate buffer at a pH level of 4.0 and a scan rate of 100 mV s^{-1} with a wide range of concentrations from 6.0×10^{-6} to 1.0×10^{-4} M. (B) Corresponding calibration curves for different concentrations. (C) DPV curves of the (i) bare GCE in PBS; (ii) bare GCE, and (iii) GCE/PEDOT:PSS in 0.01 M of PBS (at pH level of 4.0) containing 0.1 mM of FURO at a scan rate of 100 mV s^{-1}.

Table 1. Comparison Chart for the Detection of FURO Using an Electrochemical Sensor

electrode materials	linear range (μM)	detection limit (μM)	methods	supporting electrolyte	references
poly(vinyl chloride) membrane electrode	1.59×10^{-4} to 1.0×10^{-2} M	1.19×10^{-4} M	potentiometry	borate buffer (pH 9.6)	41
Au	6.0×10^{-6} to 8.0×10^{-4} M	4.12×10^{-8} M	DPV	Brinton–Robinson buffer solution	5
MWCNT-paste electrode	8.0×10^{-6} to 2.0×10^{-4} M	2.9×10^{-7} M	CV	Brinton–Robinson buffer solution	40
carbon paste electrode	5.0×10^{-7} to 10.0×10^{-6} M	4.47×10^{-9} M	DPV	BR buffer (pH 4.8)	14
MIP electrode	1.0×10^{-7} to 7.0×10^{-6} M	7.0×10^{-8} M	DPV	acetate buffer solution	42
carboxyl-MWCNT sensor	0.03 to 140.0 μg mL^{-1}	0.007 μg mL^{-1}	DPV	Britton–Robinson buffer (pH 5.7)	43
g-MnO_2/chitosan–PGE	0.05 to 4.20×10^{-6} M	3.88×10^{-9} M	SWV	acetate buffer solution	44
graphite–polyurethane	0.15–21 μM	0.15 μM	CV, DPV	acetate buffer solution (pH 3.3)	45
PEDOT:PSS/GCE	6.0×10^{-6} to 1.0×10^{-4} M	2.0×10^{-6} M	DPV	PBS (pH 4.0)	this work

electroactive area of GCE and GCE/PEDOT:PSS was found to be 0.106 and 0.257 cm^2, respectively.

Additionally, CV curves from −0.2 to 0.6 V with decreasing scan rate from outer to inner are represented in Figure 3B. It is observed that the peak current gradually decreases with minimizing the scan rate, proving the presence of an ion-transfer phenomenon that was controlled by diffusion. It can be clearly observed that the anodic and cathodic peak currents increased linearly with the scan rate, suggesting that a diffusion-controlled mass-transfer phenomenon at the solution electrode interface took place.

3.3. Electrochemical Detection of Furosemide. The electrochemical oxidation of FURO on the GCE/PEDOT:PSS-modified surface in 0.01 M PBS at pH 4.0 is shown in Scheme 2. In fact, the FURO oxidation consists of two steps, one is nitrogen free radical formation and another is for $\pi-\pi^*$ bond formations in C═N.[14,40]

Figure 4A shows that the differential pulse voltammetry (DPV) analysis of 1.0×10^{-4} M of FURO was performed in 0.01 M PBS (at pH level of 4.0) for bare GCE and GCE/PEDOT:PSS, which gradually increased the successive peak amplitude. In addition, a successful response was searched in the case of different analytic concentration ranges. In the observation of an anodic peak, it is noted that the oxidation current decreases proportionally by decreasing the concentration of FURO at the range of 6×10^{-6} to 1.0×10^{-4} M. Excellent correlations were maintained among FURO concentrations and the oxidation current. The linear concentration verses followed the regression equation of $y = 0.0236x + 0.2001$ ($R^2 = 0.9981$) with a detection limit of 2.0×10^{-6} M. This lower concentration indicates that the developed GCE/PEDOT:PSS electrochemical sensor denoted linearity and comparatively the lowest reported detection limit.

To analyze the prefeasibility of electrode modification, DPV of 1.0×10^{-6} M FURO was investigated through bare GCE and GCE/PEDOT:PSS. The result of the DPV analysis showed that GCE/PEDOT:PSS provided better electrochemical response than bare GCE as can be seen in Figure 4C.

The outcome of the current work was compared to the other reported modified electrodes for further investigation. Table 1 shows the properties of different modified electrodes and GCE/PEDOT:PSS. The GCE/PEDOT:PSS sensor showed

https://doi.org/10.1021/acsomega.3c00463
ACS Omega 2023, 8, 16851−16858

notable benefits including acceptable linear range, low detection limit, and high sensitivity.

4. SELECTIVITY, REPRODUCIBILITY, AND STABILITY STUDY

The most important parameters for evaluating the performance of the modified electrode are selectivity, reproducibility, and stability. The selectivity of the proposed sensor was done in a mixture of Na^+, K^+, Ca^+, dopamine, serotonin, oxalic acid, citric acid, sucrose, glucose, and dextrose. The 100 μM FURO detection was performed in 10-fold of this organic−inorganic mixture, but there is no significant effect (less than 1.45%). To study the reproducibility of GCE/PEDOT:PSS, a series of repetitive DPV experiments were performed using the same electrode. The deviation of the current response for various concentrations of samples was observed to be less than 1%, which indicates that GCE/PEDOT:PSS had an excellent reproducibility. The stability of GCE/PEDOT:PSS was employed under the optimized conditions of DPV and was recorded for FURO (100 μM) in 0.01 M of PBS (at a pH level of 4.0) at 100 mV s^{-1}. The DPV peak current of FURO was examined over 2 weeks and was checked every 7 days while being stored in a refrigerator at 4 °C. There was no significant change in the peak response found after 7 days of storage, indicating a good film stability of the sensor. Furthermore, a small deviation of the peak current (less than 3%) was found after 2 weeks of storage, suggesting that the proposed sensor has an excellent stability and lifetime. Hence, the proposed modified electrode has potential selectivity, reproducibility, and stability for FURO detection.

5. DETECTION OF FUROSEMIDE IN REAL SAMPLES

The applicability of the proposed GCE/PEDOT:PSS sensor for the determination of FURO in real samples such as urine, blood serum, and pharmaceutical products was examined by analytical recovery experiments. The results shown in Table 2

Table 2. Comparison of FURO in Three Different Real Sample Media

samples name	added (μM)	found (μM)	recovery (%)	RSD (%)
urine	100	99.6	99.6	0.11
blood serum	100	99.7	99.7	0.09
pharmaceutical products	100	100	100	0.001

are typical DPV responses for known FURO concentrations of urine and pharmaceutical samples. The recovery experiment was carried out by a standard addition method. The results show excellent performance in the detection of FURO with a very good recovery value of 99.6 and 100%, indicating that the proposed GCE/PEDOT:PSS sensor can be applied for the detection of different furosemide concentrations in both pharmaceuticals and urine sample with satisfactory accuracy and precision.

6. CONCLUSIONS

In this study, we have successfully developed a simple GCE/PEDOT:PSS electrochemical-based sensor for the sensitive and selective detection of FURO. The proposed sensor showed a good electrocatalytic behavior toward electrochemical oxidation of FURO at a pH level of 4.0. Hence, the fabricated GCE sensor can measure target analysts at very low FURO concentrations, showing an excellent detection limit. Moreover, the PEDOT:PSS-modified GCE showed a wide linear detection range, long-term stability, and reusability, and the response was reproducible. Finally, the proposed method with good precision and accuracy was developed for the determination of furosemide in as a real sample such as urine and pharmaceutical formulations.

AUTHOR INFORMATION

Corresponding Author

Md. Zaved Hossain Khan − *Department of Chemical Engineering and Laboratory of Nano-Bio and Advanced Materials Engineering (NAME), Jashore University of Science and Technology, Jashore 7408, Bangladesh;* orcid.org/0000-0002-4828-0203; Email: zaved.khan@yahoo.com

Authors

Md. Shamim Hossain − *Department of Chemical Engineering and Laboratory of Nano-Bio and Advanced Materials Engineering (NAME), Jashore University of Science and Technology, Jashore 7408, Bangladesh*

Md. Abdul Khaleque − *Department of Chemical Engineering and Laboratory of Nano-Bio and Advanced Materials Engineering (NAME), Jashore University of Science and Technology, Jashore 7408, Bangladesh*

Md. Romzan Ali − *Department of Chemical Engineering and Laboratory of Nano-Bio and Advanced Materials Engineering (NAME), Jashore University of Science and Technology, Jashore 7408, Bangladesh*

Md. Sadek Bacchu − *Department of Chemical Engineering and Laboratory of Nano-Bio and Advanced Materials Engineering (NAME), Jashore University of Science and Technology, Jashore 7408, Bangladesh*

Md. Ikram Hossain − *Department of Chemical Engineering and Laboratory of Nano-Bio and Advanced Materials Engineering (NAME), Jashore University of Science and Technology, Jashore 7408, Bangladesh*

Mohamed Aly Saad Aly − *Department of Electrical and Computer Engineering at Georgia Tech Shenzhen Institute (GTSI), Tianjin University, Shenzhen, Guangdong 518052, China;* orcid.org/0000-0003-0091-2467

Complete contact information is available at: https://pubs.acs.org/10.1021/acsomega.3c00463

Notes

The authors declare no competing financial interest.

REFERENCES

(1) Espinosa Bosch, M.; Ruiz Sánchez, A. J.; Sánchez Rojas, F.; Bosch Ojeda, C. Recent Developments in Analytical Determination of Furosemide. *J. Pharm. Biomed. Anal.* **2008**, *48*, 519−532.

(2) Cantarovich, F.; Galli, C.; Benedetti, L.; Chena, C.; Castro, L.; Correa, C.; Loredo, J. P.; Fernandez, J. C.; Locatelli, A.; Tizado, J. High Dose Frusemide in Established Acute Renal Failure. *Br. Med. J.* **1973**, *4*, 449−450.

(3) Mason, J.; Kain, H.; Welsch, J.; Schnermann, J.; Murdaugh, E.; Faltay, P.; Sigrid, P.; Steff, M. The early phase of experimental acute renal failure: VI. The influence of furosemide. *Pfluegers Arch.* **1981**, *392*, 125−133.

(4) Kennelly, P.; Sapkota, R.; Azhar, M.; Cheema, F. H.; Conway, C.; Hameed, A. Diuretic Therapy in Congestive Heart Failure. *Acta Cardiol.* **2022**, *77*, 97−104.

https://doi.org/10.1021/acsomega.3c00463
ACS Omega 2023, 8, 16851−16858

(5) Shetti, N. P.; Sampangi, L. V.; Hegde, R. N.; Nandibewoor, S. T. Electrochemical Oxidation of Loop Diuretic Furosemide at Gold Electrode and Its Analytical Applications. *Int. J. Electrochem. Sci.* **2009**, *4*, 104−121.
(6) Beermann, B. Kinetics and Dynamics of Furosemide and Slow-Acting Furosemide. *Clin. Pharmacol. Ther.* **1982**, *32*, 584−591.
(7) Makein, L. J. Correlation of Near-Infrared Chemical Imaging of Pharmaceutical Dosage Forms with Their Dissolution Performance. Ph.D. Thesis, University of London, University College London, UK, 2007; p 1.
(8) Vree, T. B.; van den Biggelaar-Martea, M.; Verwey-van Wissen, C. P. W. G. M. Determination of Furosemide with Its Acyl Glucuronide in Human Plasma and Urine by Means of Direct Gradient High-Performance Liquid Chromatographic Analysis with Fluorescence Detection Preliminary Pharmacokinetics and Effect of Probenecid. *J. Chromatogr. B: Biomed. Sci. Appl.* **1994**, *655*, 53−62.
(9) Eid, P. S.; Ibrahim, D. A.; Zayan, A. H.; Mahmoud, M.; Elrahman, A. Comparative Effects of Furosemide and Other Diuretics in the Treatment of Heart Failure: A Systematic Review and Combined Meta-Analysis of Randomized Controlled Trials. *Heart Failure Rev.* **2021**, *26*, 127−136.
(10) Luis, M. L.; Fraga, J. M. G.; Jiménez, A. I.; Jiménez, F.; Hernández, O.; Arias, J. J. Application of PLS Regression to Fluorimetric Data for the Determination of Furosemide and Triamterene in Pharmaceutical Preparations and Triamterene in Urine. *Talanta* **2004**, *62*, 307−316.
(11) Solich, P.; Sklenářová, H.; Polášek, M.; Karlíček, R. Application of Flow Injection Technique in Pharmaceutical Analysis. Part I: Spectrophotometric and Chemiluminescence Detection. *Pharmaceuticals* **2001**, *50*, 39. No. January
(12) Billalli, H. B.; Sharanabasamma, K.; Tuwar, S. M. Mechanism of the Osmium(VIII)-Catalysed Oxidation of Fursemide by Alkaline Hexacyanoferrate(Iii) and Analysis of Fursemide by a Kinetic and Catalytic Method. *Prog. React. Kinet. Mech.* **2010**, *35*, 347−367.
(13) Barroso, M. B.; Jiménez, R. M.; Alonso, R. M.; Ortiz, E. Determination of Piretanide and Furosemide in Pharmaceuticals and Human Urine by High-Performance Liquid Chromatography with Amperometric Detection. *J. Chromatogr. B: Biomed. Sci. Appl.* **1996**, *675*, 303−312.
(14) Bukkitgar, S. D.; Shetti, N. P. Electrochemical Oxidation of Loop Diuretic Furosemide in Aqueous Acid Medium and Its Analytical Application. *Cogent Chem.* **2016**, *2*, 1152784.
(15) Rao, Y.; Zhang, X.; Luo, G.; Baeyens, W. R. G. Chemiluminescence Flow-Injection Determination of Furosemide Based on a Rhodamine 6G Sensitized Cerium (IV) Method. *Anal. Chim. Acta* **1999**, *396*, 273−277.
(16) Baranowska, I.; Markowski, P.; Gerle, A.; Baranowski, J. Determination of Selected Drugs in Human Urine by Differential Pulse Voltammetry Technique. *Bioelectrochemistry* **2008**, *73*, 5−10.
(17) Serp, P. 7.13 Carbon. In *Comprehensive Inorganic Chemistry II*; Elsevier, 2013.
(18) Elschner, A.; Kirchmeyer, S.; Lovenich, W.; Merker, U.; Reuter, K. *PEDOT*; CRC Press, 2010.
(19) Nardes, A. M.; Kemerink, M.; de Kok, M. M.; Vinken, E.; Maturova, K.; Janssen, R. A. J. Conductivity, Work Function, and Environmental Stability of PEDOT:PSS Thin Films Treated with Sorbitol. *Org. Electron.* **2008**, *9*, 727−734.
(20) Bano, N.; Zaman, S.; Zainelabdin, A.; Hussain, S.; Hussain, I.; Nur, O.; Willander, M. ZnO-Organic Hybrid White Light Emitting Diodes Grown on Flexible Plastic Using Low Temperature Aqueous Chemical Method. *J. Appl. Phys.* **2010**, *108*, 043103.
(21) Ouyang, J.; Xu, Q.; Chu, C. W.; Yang, Y.; Li, G.; Shinar, J. On the Mechanism of Conductivity Enhancement in Poly(3,4-Ethylenedioxythiophene):Poly(Styrene Sulfonate) Film through Solvent Treatment. *Polymer* **2004**, *45*, 8443−8450.
(22) Kim, Y.; Yoo, S.; Kim, J. H. Water-Based Highly Stretchable PEDOT:PSS/Nonionic WPU Transparent Electrode. *Polymers* **2022**, *14*, 949.
(23) Otero, T. F.; Martinez, J. G.; Hosaka, K.; Okuzaki, H. Electrochemical Characterization of PEDOT-PSS-Sorbitol Electrodes. Sorbitol Changes Cation to Anion Interchange during Reactions. *J. Electroanal. Chem.* **2011**, *657*, 23−27.
(24) Liu, J.; Agarwal, M.; Varahramyan, K. Glucose Sensor Based on Organic Thin Film Transistor Using Glucose Oxidase and Conducting Polymer. *Sens. Actuators, B* **2008**, *135*, 195−199.
(25) Silva, F. A. R.; Silva, L. M.; Ceschin, A. M.; Sales, M. J. A.; Moreira, S. G. C.; Viana, C. E. KDP/PEDOT:PSS Mixture as a New Alternative in the Fabrication of Pressure Sensing Devices. *Appl. Surf. Sci.* **2008**, *255*, 734−736.
(26) Mu, P.; Zhang, H.; Jiang, H.; Dong, T.; Zhang, S.; Wang, C.; Li, J.; Ma, Y.; Dong, S.; Cui, G. Bioinspired Antiaging Binder Additive Addressing the Challenge of Chemical Degradation of Electrolyte at Cathode/Electrolyte Interphase. *J. Am. Chem. Soc.* **2021**, *143*, 18041−18051.
(27) Hareesh, K.; Shateesh, B.; Joshi, R. P.; Dahiwale, S. S.; Bhoraskar, V. N.; Haram, S. K.; Dhole, S. D. PEDOT:PSS Wrapped NiFe2O4/RGO Tertiary Nanocomposite for the Super-Capacitor Applications. *Electrochim. Acta* **2016**, *201*, 106−116.
(28) Manjakkal, L.; Pullanchiyodan, A.; Yogeswaran, N.; Hosseini, E. S. A Wearable Supercapacitor Based on Conductive PEDOT : PSS-Coated Cloth and a Sweat Electrolyte. *Adv. Mater.* **2020**, *32*, 1907254.
(29) Mu, P.; Zhang, H.; Dong, T.; Jiang, H.; Zhang, S.; Wang, C.; Li, J.; Dong, S.; Cui, G. A Melatonin-Inspired Coating as an Electrolyte Preservative for Layered Oxide Cathode-Based Lithium Batteries. *Chem. Eng. J.* **2022**, *437*, 135032.
(30) Wang, C.; Ma, Y.; Du, X.; Zhang, H.; Xu, G.; Cui, G. A Polysulfide Radical Anions Scavenging Binder Achieves Long-life Lithium−Sulfur Batteries. *Battery Energy* **2022**, *1*, 20220010.
(31) Kim, J. H.; Choi, H. J.; Kim, H. K.; Lee, S. H.; Lee, Y. H. A Hybrid Supercapacitor Fabricated with an Activated Carbon as Cathode and an Urchin-like TiO2 as Anode. *Int. J. Hydrogen Energy* **2016**, *41*, 13549−13556.
(32) Kim, H.; Lee, Y.; Park, G.; Park, S.; Choi, Y.; Yoo, Y. Fabrication of Carbon Paper Containing PEDOT : PSS for Use as a Gas Diffusion Layer in Proton Exchange Membrane Fuel Cells. *Carbon* **2015**, *85*, 422−428.
(33) Hassan, G.; Sajid, M.; Choi, C. Highly Sensitive and Full Range Detectable Humidity Sensor Using PEDOT : PSS , Methyl Red and Graphene Oxide Materials. *Sci. Rep.* **2019**, *9*, 15227.
(34) K.Chatap, V.; L. Patil, P.; D. Patil, S. In-Vitro , Ex-Vivo Characterization of Furosemide Bounded Pharmacosomes for Improvement of Solubility and Permeability. *Adv. Pharmacol. Pharm.* **2014**, *2*, 67−76.
(35) Benoudjit, A.; Bader, M. M.; Wan Salim, W. W. A.; Wan, A. Study of Electropolymerized PEDOT : PSS Transducers for Application as Electrochemical Sensors in Aqueous Media. *Sens. Bio-Sens. Res.* **2018**, *17*, 18−24.
(36) Wustoni, S.; Saleh, A.; El-demellawi, J. K.; Koklu, A.; Hama, A.; Druet, V.; Wehbe, N.; Zhang, Y.; Inal, S. MXene Improves the Stability and Electrochemical Performance of MXene Improves the Stability and Electrochemical Performance of Electropolymerized PEDOT Films. *APL Mater.* **2020**, *8*, 121105.
(37) Banerji, A.; Kirchmeyer, S.; Meerholz, K.; Scharinger, F. Teaching Organic Electronics - Part II : Quick & Easy Synthesis of the (Semi-) Conductive Polymer PEDOT : PSS in a Snap-Cap Vial. *World J. Chem. Educ.* **2019**, *7*, 166−171.
(38) Khan, M. Z. H.; Ahommed, M. S.; Daizy, M. Detection of Xanthine in Food Samples with an Electrochemical Biosensor Based on PEDOT : PSS and Functionalized Gold Nanoparticles. *RSC Adv.* **2020**, *10*, 36147−36154.
(39) Ali, M. R.; Bacchu, M. S.; Daizy, M.; Tarafder, C.; Hossain, M. S.; Rahman, M. M.; Khan, M. Z. H. A Highly Sensitive Poly-Arginine Based MIP as an Electrochemical Sensor for Selective Detection of Dimetridazole. *Anal. Chim. Acta* **2020**, *1121*, 11−16.
(40) Malode, S. J.; Abbar, J. C.; Shetti, N. P.; Nandibewoor, S. T. Voltammetric Oxidation and Determination of Loop Diuretic

https://doi.org/10.1021/acsomega.3c00463
ACS Omega 2023, 8, 16851−16858

Furosemide at a Multi-Walled Carbon Nanotubes Paste Electrode. *Electrochim. Acta* **2012**, *60*, 95−101.
(41) Tescarollo Dias, I. L.; de Oliveira Neto, G.; Vendramini, D. C. A Poly (Vinyl Chloride) Membrane Electrode for the Determination of the Diuretic Furosemide. *Anal. Lett.* **2004**, *37*, 35−46.
(42) Kor, K.; Zarei, K. Development and characterization of an electrochemical sensor for furosemide detection based on electro-polymerized molecularly imprinted polymer. *Talanta* **2016**, *146*, 181−187.
(43) Heidarimoghadam, R.; Farmany, A. Rapid Determination of Furosemide in Drug and Biological Fluids by a Carboxyl-MWCNT Sensor. *Mater. Sci. Eng., C* **2016**, *58*, 1242−1245.
(44) Said, M. I.; Rageh, A. H.; Abdel-aal, F. A. M. Fabrication of Novel Electrochemical Sensors Based on Modi Fi Cation with Di Ff Erent Polymorphs of MnO 2 Nanoparticles . Application to Furosemide Analysis In Pharmaceutical and Urine Samples. *RSC Adv.* **2018**, *8*, 18698−18713.
(45) Semaan, F. S.; Pinto, E. M.; Cavalheiro, E. T. G.; Brett, M. A. A Graphite-Polyurethane Composite Electrode for the Analysis of Furosemide. *Electroanalysis* **2008**, *20*, 2287−2293.

https://doi.org/10.1021/acsomega.3c00463
ACS Omega 2023, 8, 16851−16858